Preprints.org

Article

Not peer-reviewed version

Development of a Korean Sign Language Translation System Using Knitted Strain Sensor-Integrated Smart Gloves

Youn-Hee Kim * and You-Kyung Oh

Posted Date: 16 June 2025

doi: 10.20944/preprints202506.1182.v1

Keywords: Knitted strain sensors; Plain plated stitch; Smart glove; Korean Sign Language; Textile integration system

Preprints.org is a free multidisciplinary platform providing preprint service that is dedicated to making early versions of research outputs permanently available and citable. Preprints posted at Preprints.org appear in Web of Science, Crossref, Google Scholar, Scilit, Europe PMC.

Copyright: This open access article is published under a Creative Commons CC BY 4.0 license, which permit the free download, distribution, and reuse, provided that the author and preprint are cited in any reuse.

Preprints.org (www.preprints.org) | NOT PEER-REVIEWED | Posted: 16 June 2025 doi:10.20944/preprints202506.1182.v1

Disclaimer/Publisher's Note: The statements, opinions, and data contained in all publications are solely those of the individual author(s) and contributor(s) and not of MDPI and/or the editor(s). MDPI and/or the editor(s) disclaim responsibility for any injury to people or property resulting from any ideas, methods, instructions, or products referred to in the content.

Article

Development of a Korean Sign Language Translation System Using Knitted Strain Sensor-Integrated Smart Gloves

Youn-Hee Kim [1]* and You-Kyung Oh [1]

Department of Convergence Design and Technology, Kookmin University, Seoul 02707, Republic of Korea; shell62@kookmin.ac.kr (Y.-H.K.); fbdk96@kookmin.ac.kr (Y.-K.O.)

* Correspondence: shell62@kookmin.ac.kr

Abstract: Herein, an integrated system is developed based on knitted strain sensors for real-time translation of sign language into text and audio voices. To investigate how the structural characteristics of the knit affect the electrical performance, the position of the conductive yarn and the presence or absence of elastic yarn are set as experimental variables, and five distinct sensors are manufactured. A comprehensive analysis of the electrical and mechanical performance, including sensitivity, responsiveness, reliability, and reproducibility, reveals that the sensor with a plain plated knit structure, no elastic yarn included, and the conductive yarn positioned uniformly on the back exhibits the best performance, with a gauge factor (GF) of 88. The sensor demonstrates high sensitivity and a fast response speed to finger joint bending. Additionally, it exhibits stable reproducibility and reliability across various angles and speeds, thereby confirming its optimized characteristics for sign language recognition. Based on this design, an integrated textile-based system is developed by incorporating the sensor, interconnections, snap connectors, and a microcontroller unit (MCU) with built-in Bluetooth Low Energy (BLE) technology into the knitted glove. The completed system successfully recognizes 12 Korean Sign Language (KSL) gestures in real time and outputs them as text and audio voices in conjunction with a dedicated application. Thus, the present study quantitatively elucidates the structure-performance relationship of a knitted sensor and proposes a wearable system that accounts for real-world usage environments, thereby demonstrating the commercialization potential of the technology.

Keywords: Knitted strain sensors; Plain plated stitch; Smart glove; Korean Sign Language; Textile integration system

1. Introduction

Humans have used not only voice, but also facial expressions, body movements, and hand gestures to communicate accurately and effectively [1]. In particular, hand gestures have a wide variety of expressive forms, and have long been used as a means of communicating at the sentence level when opinions cannot be expressed through spoken language. Signed languages are conveyed by the hands, face, and body, and are primarily perceived visually [2]. However, without prior knowledge of sign language, it is difficult for non-signers to receive and understand this conversational communication. This creates a communication barrier between signers and non-signers [3]. To address this issue, there is a growing need for technologies that can recognize sign language and convert it into visual or auditory information.

Knitted strain sensors are lightweight, flexible, and highly elastic, which makes them comfortable to wear for extended periods [4]. They can continuously monitor biosignals such as breathing and movement, thereby positioning them as key materials for human interface technologies. In particular, their excellent stretchability allows them to detect both small and large movements, which makes them well suited for monitoring finger joint motion. Based on these

© 2025 by the author(s). Distributed under a Creative Commons CC BY license.

Preprints.org (www.preprints.org) | NOT PEER-REVIEWED | Posted: 16 June 2025 doi:10.20944/preprints202506.1182.v1

characteristics, the active development of knitted smart gloves for hand gesture recognition has been actively pursued in recent years. For instance, Ryu et al. [5] used a knitted glove sensor to analyze the electrical resistance behavior under compressive and tensile strains according to finger movements. The proposed sensor maintained excellent electrical properties and stability even after more than 400 repeated external deformations and five normal washing processes. Heo et al. [6] demonstrated a textile-based silver nanowire (AgNW) sensor with high conductivity (434.7 S/cm) on a polyester-based spandex substrate by utilizing stretchable and flexible polydimethylsiloxane (PDMS) films as both the interface/planarization and passivation layers. For hand gesture recognition, a full-sized glove-type sensor integrating five strain sensor units was designed, and it showed stable electrical responses to each finger movement. Lee et al. [7] fabricated sensors using the intarsia technique for hand posture pattern recognition and integrated them into a knitted glove. The proposed sensor exhibited a gauge factor (GF) of 12 at a maximum strain of 10%, and classification of 10 hand postures from 10 subjects was achieved with an average accuracy of 94.17%. Similarly, Han et al. [8] used the intarsia technique to fabricate sensors with silver-plated nylon and nylon/spandex yarns. Considering the effects of elastic materials, sensor size, and glove size on performance, the optimal sensor was integrated into the glove. Tests on nine numeric gestures demonstrated that the proposed glove system provided stable recognition performance. Further, Qin et al. [9] developed a fabric sensor based on Ecoflex/carbon composite ink, which exhibited a high linear resistance change rate ($R^2 = 0.9965$) over a strain range of 0–100%. In addition, it maintained excellent durability even after 2,000 cycles of repeated stretching. This intelligent fabric sensor demonstrated the potential for human–computer interaction by monitoring finger movements. Cheng et al. [10] developed a flexible strain sensor using piezoresistive knitted fabrics and polydimethylsiloxane (PDMS), and evaluated its performance by attaching it to various body parts, including the fingers, wrist, upper arm, and thigh. The sensor demonstrated reliable detection of human movements, with a strain range of 0–87%, a gauge factor (GF) between 3.7 and 10.6, stable responsiveness, and excellent durability.

While the abovementioned studies have demonstrated the capability of textile-based sensors to detect finger movements and their implementation in smart glove systems, the effects of various knitted structures on the electrical performance of these sensors have not been thoroughly investigated. Knitted fabrics have a structural mechanism in which the shape of the loops changes during the stretching and recovery processes, thus causing variations in the contact points between yarns [11]. This directly affects key sensor performance metrics such as sensitivity, responsiveness, reliability, and reproducibility. Therefore, prior to integrating sensors into smart gloves, performance optimization based on knitted structural characteristics is essential for accurately detecting finger joint movements. This requires a comprehensive investigation of how factors such as knitting techniques, knit structures, and material combinations influence the electrical properties of the sensors. Moreover, studies on system-level integration for real-world applications remain limited. The entire process from sensor design to signal interface to final output must be organically configured, and a design that reflects the actual use environment is required. Accordingly, the objectives of this study are to: (1) conduct an in-depth analysis of how the structural characteristics of knitted sensors affect their electrical performance; (2) design and fabricate high-performance sensors optimized for finger joint motion detection; and (3) develop a fully integrated textile-based system suitable for practical implementation in smart gloves.

In a previous study [12], the sensing characteristics of knitted strain sensors were analyzed based on knitting parameters such as stitch pattern, needle position (NP) number, and number of yarns. It was found that the plain stitch pattern, NP 12, and single-strand configuration were most effective for detecting subtle movements. Building on these findings, the present study maintains the same knitting conditions and conducts a detailed comparison of sensor performance based on two variables: the placement of the conductive yarn and the presence or absence of elastic yarn. Five distinct sensor types were fabricated and subjected to 1,000 bending cycles, with performance evaluated across different angles and speeds. Key performance indicators—including sensitivity, responsiveness, reliability, and reproducibility—were used to identify the optimal configuration for recognizing finger joint movements. The selected sensor was then integrated into a glove to evaluate its real-time recognition of 12 Korean Sign Language (KSL) consonant and vowel gestures.

© 2025 by the author(s). Distributed under a Creative Commons CC BY license.

Preprints.org (www.preprints.org) | NOT PEER-REVIEWED | Posted: 16 June 2025 doi:10.20944/preprints202506.1182.v1

Additionally, a mobile application was developed to convert recognized gestures into both text and voice output, thereby demonstrating the practical feasibility and scalability of the proposed sign language recognition system.

2. Materials and Methods

2.1. Knit Structure and Sensing Mechanism

Knitted fabric is formed by vertically interconnected loops of a single continuous yarn. Structurally, it is composed of vertical wales and horizontal courses [13], [14], with each loop consisting of three segments: the head, leg, and sinker [15]. Knitted structures are created in various forms using the loop as a fundamental unit. Importantly, Holm-type electrical contacts are generated when the head of one loop comes into contact with the sinker of an adjacent loop. When the knit is stretched in the wale direction, the contact surface and pressure between the head and sinker increase, the gap between loops narrows, and the number of contact points increases. As a result, a negative piezoresistive effect occurs, thereby lowering the resistance during stretching [16].

Based on this mechanism, the present study examines the electrical resistance behavior of knitted strain sensors under mechanical deformation. Two experimental variables are considered: (1) the placement of the conductive yarn and (2) the inclusion of elastic yarn. To assess the effect of conductive yarn placement on loop contact points and conductive pathway formation, plain plated and plain assembled knit structures are compared. Additionally, the role of elastic yarn in modulating structural contact and pressure is analyzed by comparing two material configurations: normal yarn–conductive yarn and elastic yarn–conductive yarn combinations.

2.2. Knitted Sensor Fabrication

The knitted strain sensors were designed by adjusting variables such as sensor size, NP number, and loop location using the M1 Plus 7.2.037 pattern software. The sensors were then fabricated using a CMS330 KI W TT SPORT E7.2 (14-gauge) computerized flat knitting machine (STOLL, Reutlingen, Germany). The plain plated knit and plain assembled knit structures were then fabricated based on different knitting techniques [17]. Specifically, the plain plated knit is composed of two types of yarn, and is characterized by loops arranged in parallel on the front and back sides. In the present study, this structure was made by combining non-conductive and conductive yarns. To ensure uniform distribution of the conductive yarn on either the front or back side of the fabric, the intarsia yarn carrier and plating yarn carrier were used separately. This method enabled consistent placement of the conductive yarn on a specific surface of the sensor. Meanwhile, the plain assembled knit is a structure in which two or more yarns are combined into a single loop. In contrast, the plain assembled knit combines two strands of yarn—here, conductive and non-conductive—into a single loop using a single intarsia yarn carrier. Due to the twisting interaction between yarns during the knitting process, the conductive yarn was randomly distributed on both the front and back sides of the fabric. This led to a non-uniform and irregular distribution of the conductive material throughout the sensor.

Table 1. Photographic images and experimental characterizations of the knitted strain sensor samples.

sample code	Pt-b-A/W		Pt-f-A/W		As-f-A/W		As-b-A/W		Pt-b-R/N/P/W	
structure	plated		plated		assembled		assembled		plated	
conductive yarn position	back side		front side		mainly front side		mainly back side		back side	
	front	back	front	back	front	back	front	back	front	back
photographic image	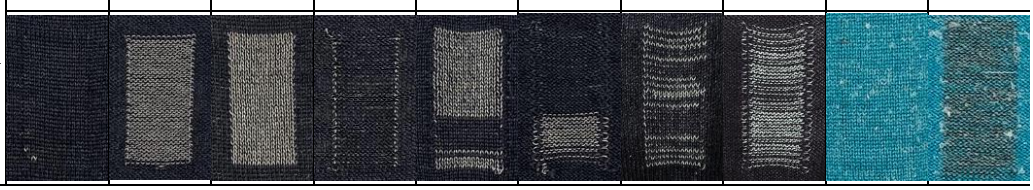									

© 2025 by the author(s). Distributed under a Creative Commons CC BY license.

Preprints.org (www.preprints.org) | NOT PEER-REVIEWED | Posted: 16 June 2025 doi:10.20944/preprints202506.1182.v1

yarn composition	2-ply A/W 1:1 ratio+ conductive yarn	3-ply R/N/P/W 42:20:10:28 ratio+ span + conductive yarn

The five fabricated sensor samples, produced using two different knitting techniques, are summarized in Table 1. The samples were produced with the plated (Pt) structure or with the assembled (As) structure, wherein the conductive yarn was distributed on either the back (b) or front (f) sides. For the As samples, where the conductive yarn distribution is inherently random due to the simultaneous feeding of yarns, the designation of "front" or "back" was determined based on the surface exhibiting a higher concentration of conductive yarn. **Additionally**, to investigate the effect of elasticity, two types of non-conductive yarns were used. In four of the samples, a non-elastic insulating layer was applied, consisting of a single strand of 2-ply blended yarn made from acrylic (A) and wool (W) in a 1:1 ratio, supplied by C&TEX (Seoul, Republic of Korea). In contrast, one sample included an elastic insulating layer, composed of two strands of 3-ply blended yarn containing rayon (R), nylon (N), polyester (P), and wool (W) in a 42:20:10:28 ratio, along with a single strand of spandex (SPAN) yarn. This yarn was also provided by C&TEX. All five samples had the same overall dimensions of 90 mm × 140 mm. The actual sensing area of the knitted strain sensor was designed to be 20 mm × 40 mm, based on the typical surface area of a finger joint. The conductive yarn used in each sensor was a polyamide (PA), polyester(P) blend (<530 Ω/m) manufactured by AMANN (Bönnigheim, Germany).

For electrical connectivity to the hardware, a lock stitch was employed for the signal line, and a snap fastener was used as the ground (GND) terminal. The interconnection line was fabricated using silver-coated PA/P conductive yarn from AMANN (Bönnigheim, Germany), which has a relatively low resistance of <85 Ω/m. Taking the fabric's elasticity into account, the interconnection lines were sewn in a zigzag pattern with an approximate spacing of 3 mm to maintain flexibility. Two interconnection lines were routed from points 5 mm inside the top and bottom edges of the sensor to the GND terminal. Snap connectors with a diameter of 5 mm were attached at the ends of these lines to facilitate coupling with the external hardware system.

2.3. Experimental Setup for Performance Evaluation

As detailed in the following paragraphs, dynamic bending tests were initially performed in order to optimize the knitted strain sensors for response to finger movements, after which the optimized sensor was integrated into a glove and its motion recognition performance was evaluated by user testing.

2.3.1. Repetitive Bending Test

Dynamic bending tests were performed to verify whether the sensors could recognize complex finger movements and provide consistent measurements. The electrical characteristics of the sensors were evaluated using an E-textile flexing tester (CKFT-T400, Netest, Hwasung-si, Republic of Korea). Prior to testing, each sample was subjected to 5 pre-bending cycles to ensure stable and uniform electrical signals [18]. The dynamic bending tests were performed for 1,000 cycles each, with bending angles of 30°, 60°, and 90° at speeds of 10, 30, and 50 cycles per minute (cpm). The collected data were analyzed to assess the sensitivity, responsiveness, reliability, and reproducibility of the sensor.

2.3.2. KSL Smart Glove Motion Recognition Test

The selected sensor was integrated into the KSL smart glove in order to evaluate the possibility of fingerspelling recognition via user tests. Fingerspelling is a method of expressing Korean consonants and vowels by using the shapes of the hand and fingers to supplement vocabulary that is difficult to express in sign language [19]. KSL fingerspelling consists of a total of 24 characters, made up of 14 consonants and 10 vowels [20]. In this study, experiments were conducted on 10 consonants (ㄱ, ㄹ, ㅁ, ㅂ, ㅅ, ㅇ, ㅈ, ㅊ, ㅋ, and ㅎ) and 2 vowels (ㅏ and ㅣ) in KSL that can be distinguished by fingerspelling with the knitted strain sensor. Each gesture was held for 5 s in both

© 2025 by the author(s). Distributed under a Creative Commons CC BY license.

Preprints.org (www.preprints.org) | NOT PEER-REVIEWED | Posted: 16 June 2025 doi:10.20944/preprints202506.1182.v1

the initial state (no bending) and the KSL motion state (bending), and the changes in sensor output were observed.

2.4. Fabrication of the KSL Glove

In this study, a smart glove was fabricated as an interface device to facilitate communication between sign language users and non-users. The main body of the glove was knitted using two strands of A/W regular yarn. For improved wearability, the back and palm of the hand areas were constructed using a plain knit structure, while the wrist area was knitted in a 2×1 rib structure. Furthermore, the glove was custom-fitted to the user's hand size to ensure accurate stretching during finger flexion.

A 20 mm × 40 mm knitted strain sensor was fabricated by combining conductive yarn (< 530 Ω/m) with the insulating A/W yarn. The sensor was positioned at the center of the proximal interphalangeal (PIP) joint of each finger. The interconnection lines were stitched using conductive yarn (< 85 Ω/m) in a zigzag pattern with approximately 3 mm spacing. To independently detect the motion of each finger, two signal lines were added per finger. These lines started from the upper and lower edges of each sensor, at an internal offset of 0.5 mm, and extended to the GND terminal area. A total of 10 snap connectors were attached to the ends of the signal lines to interface with the hardware.

© 2025 by the author(s). Distributed under a Creative Commons CC BY license.

Preprints.org (www.preprints.org) | NOT PEER-REVIEWED | Posted: 16 June 2025 doi:10.20944/preprints202506.1182.v1

2.5. Data Acquisition and Signal Processing

Data acquisition from the sensor and glove was performed using a microcontroller unit (MCU) based on Arduino (ESP32-PICO-V3, Indifrog, Seongnam-si, Republic of Korea). The reference voltage was set to 3.3 V, and a fixed resistance of 100 Ω was used. During repeated bending and recovery motions, the electrical signals from the sensor were output to the serial monitor at 0.1 s intervals via an Arduino program. The MCU converted the sensor's deformation into digital voltage values ranging from 0 to 4095 V. To verify the real-time KSL gesture recognition capability of the smart glove, a smartphone application was developed. Sensor data were transmitted via Bluetooth Low Energy (BLE), thereby allowing finger movement information to be displayed as text and voice on the mobile device.

3. Results and Discussion

3.1. Deformation Mechanism of Five Types of Knitted Strain Sensors

The structural changes in the contact points formed between the conductive yarns during stretching and recovery for each of the five distinct sensors are revealed by the 3D modeling images in Figure 1. When bent, the sensors are stretched along the wale direction, which changes the contact positions between the conductive yarns [21]. These contact points can be classified into interlocking contacts, where physical contact occurs, and jamming contacts, where contact does not occur. The various contact points are labeled as follows: yellow (CP1) indicates contact between the loop head and sinker loop, green (CP2) indicates contact between sinker loops, red (CP3) indicates contact between loop heads, and pink (CP4) indicates contact between loop legs.

The changes in contact points before and after stretching for Pt-b-A/W are shown in Figure 1a. Before stretching, interlocking contacts (CP1, CP2, and CP4) and a jamming contact (CP3) are seen to coexist. After 10% strain, however, the CP1, CP2, CP3, and CP4 contacts have all transitioned into interlocking contacts. By contrast, the Pt-f-A/W exhibits interlocking contacts (CP1 and CP4) and jamming contacts (CP2 and CP3) before stretching (Figure 1b). Moreover, while all of these contacts have switched to jamming contacts at 10% strain, they are seen to have reverted to interlocking contacts and jamming contacts at 20% strain. The same contact point changes are observed for As-f-A/W in Figure 1c. However, because the conductive yarns are randomly arranged front and back, the number of contact points is relatively lower than Pt-f-A/W. Meanwhile, As-b-A/W (Figure 1d) exhibits the same contact point changes as Pt-b-A/W, but with a reduced number of contact points due to the irregular arrangement of yarns. Finally, Pt-b-R/N/P/W (Figure 1e) has the same structure as Pt-b-A/W, but exhibits different contact point changes due to the use of elastic yarns. The high elasticity causes high pressure to be applied between loops before stretching, and structural deformation progresses slowly during stretching, thus resulting in minimal changes in the number of contact points. This structural analysis helps to understand the differences in sensing mechanisms depending on the arrangement of conductive yarns and the presence or absence of elastic yarns, thus providing foundational data for the electrical characterization.

© 2025 by the author(s). Distributed under a Creative Commons CC BY license.

Preprints.org (www.preprints.org) | NOT PEER-REVIEWED | Posted: 16 June 2025 doi:10.20944/preprints202506.1182.v1

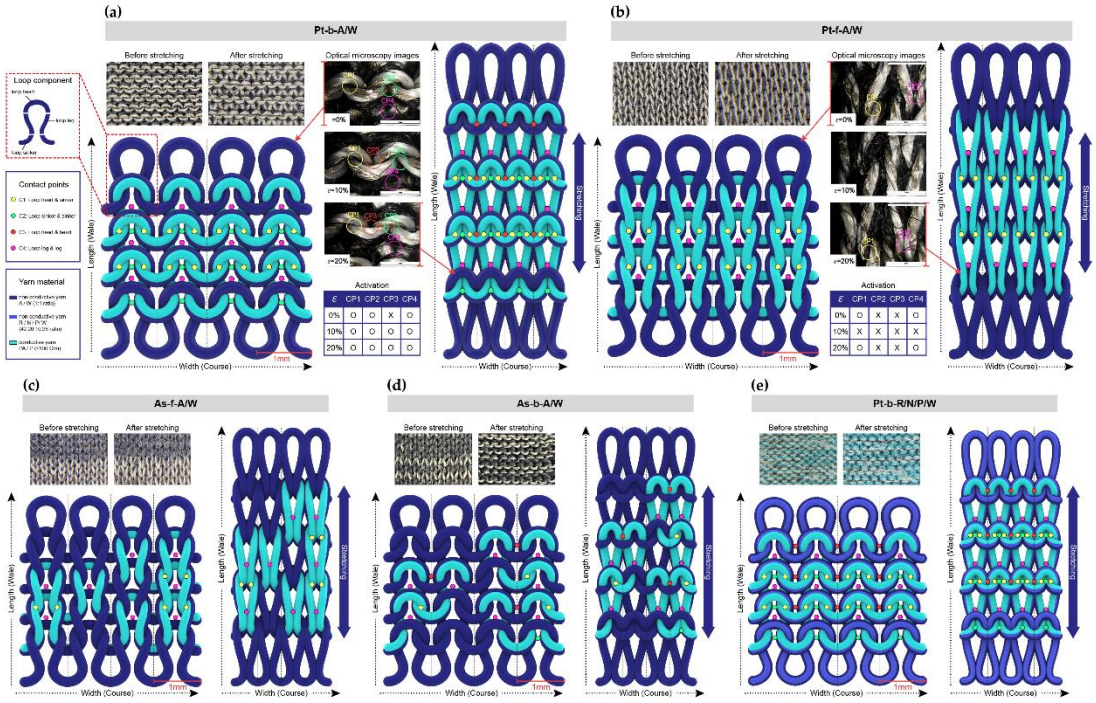

Figure 1. An analysis of the deformation mechanisms in terms of the formation of contact points before and after stretching for (a) the Pt-b-A/W; (b) the Pt-f-A/W; (c) the As-f-A/W; (d) the As-b-A/W; and (e) the Pt-b-R/N/P/W.

3.2. Dynamic Bending Test Results

3.2.1. The Bending Test Results and Initial Analysis for All Five Samples

The dynamic bending test results for all five samples are presented in Figure 2a. Here, Pt-b-A/W exhibits the largest voltage change, thereby demonstrating that the knit structure is a key factor influencing the output voltage of the strain sensor. Based on the bending test data, the corresponding strain data at 30 cpm are presented in Figure 2b. Here, one cycle has been extracted from the same section of each sample to analyze the resistance change pattern according to strain. Notably, Pt-b-A/W exhibits the largest resistance change rate, with a linear increase in resistance as the strain increases from 7% to 30%. Meanwhile, Pt-f-A/W exhibits an initial increase in resistance as the strain is increased up to 10%, followed by a decrease until 20% strain, and then an increase again at strains of up to 45%. Similarly, As-f-A/W exhibits an initial increase in resistance at strains of up to 5%, followed by a decrease until 10% strain, and then another increase at strains of up to 37.5%. By contrast, As-b-A/W exhibits a sharp increase in resistance at strains of up to 4%, followed by a more gradual increase at strains of up to 10%, after which the resistance continues to increase even more rapidly at strains of up to 32.5%, thus resulting in the second-highest resistance change after Pt-b-A/W. Finally, Pt-b-R/N/P/W exhibits an increase in resistance at strains of up to 13%, followed by a decrease at strains of up to 18%, and then another increase at strains of up to 39.5%. Thus, in brief, the Pt-f-A/W, As-f-A/W, and Pt-b-R/N/P/W each exhibit nonlinear behavior, with the resistance values both increasing and decreasing with the increase in strain, rather than exhibiting a consistent increase. Meanwhile, As-b-A/W exhibits a continual increase, but with a variable rate of change, while Pt-b-A/W exhibits a large resistance change along with a linear response to strain. These results are consistent with the abovementioned contact point changes during structural deformation. The Pt-b-A/W, which has the greatest and most steadily increasing number of contact points, shows the best sensor performance, while the other samples each exhibit irregular increases in contact points and relatively unstable resistance changes. The GF value of each sample are calculated by using Equations (1):

© 2025 by the author(s). Distributed under a Creative Commons CC BY license.

Preprints.org (www.preprints.org) | NOT PEER-REVIEWED | Posted: 16 June 2025 doi:10.20944/preprints202506.1182.v1

$$\mathrm{GF} = \frac{\frac{\Delta R}{R_0}}{\frac{\Delta L}{L_0}} = \frac{\Delta R}{\varepsilon R_0} \quad (1)$$

where R_0 is the min resistance, ΔR is the applied resistance, L_0 is the initial length, ΔL is the applied length, and ε is the strain value and the results are presented in Figure 2c. Because the knitted strain sensors used herein each exhibit a negative piezoresistive effect, whereby the resistance decreases with increased stretching, the GF was calculated by taking the initial resistance value as the maximum and the resistance after stretching as the minimum [23]. To measure small movements such as those of the fingers, sensors with high sensitivity even within a low working range are required. In this respect, although the Pt-b-A/W exhibits the narrowest working range among the five samples, it has a GF of up to ~ 89 times that of the other samples. These results clearly demonstrate that differences in the knit structure significantly affect the sensor's electrical performance, including its sensitivity, working range, and linearity of resistance change. Accordingly, a further in-depth analysis was conducted in order to determine whether the best-performing sample (i.e., the Pt-b-A/W) is suitable for monitoring complex and continuous finger bending motions.

3.2.2. In-Depth Analysis of the Bending Test Results for the Pt-b-A/W

The voltage changes of the Pt-b-A/W at a fixed bending angle of 90° under various bending speeds of 10, 30, and 50 cpm are shown in Figure 2d. Here, the output signals are seen to be stable across the various bending speeds. This indicates that the sensor can reliably detect finger movements at various speeds with consistent performance. Further, the voltage responses of the Pt-b-A/W during the initial, middle, and final stages of bending to 90° at 30 cpm for 1000 cycles (with one cycle extracted from each stage) are shown in Figure 2e. This enables an observation of the change in sensor responsiveness over time. Specifically, the sensor's response speed is evaluated by measuring the loading (bending) and unloading (recovery) times during each cycle. At 30 cpm, one cycle takes an average of 2 s. Thus, during the initial stage, the Pt-b-A/W exhibits a loading time of 0.6 s and an unloading time of 0.5 s. In the middle and final stages, the loading time of 0.7 s and an unloading time of 0.6 s. Although the loading and unloading times show a difference of 0.1 s each compared to the initial stage, they remain consistent throughout the middle and final stages, thereby confirming that the operation is completed within 2 s. In other words, despite a slight delay compared to the initial stage, the response stabilizes as the cycles repeat, thereby suggesting that the sensor can measure repetitive movements in real time. The voltage response of the Pt-b-A/W during 1000 cycles of dynamic bending to angles of 30°, 60°, and 90° at a fixed speed of 50 cpm is shown in Figure 2f. Thus, at 30° bending (red line), the average minimum voltage is seen to be 46.5% higher than that at 60° bending (purple line), while the average minimum voltage at 60° bending is 30.5% higher than that at 90° bending (blue line). These changes in voltage according to the bending angle demonstrate that the sensor is able to provide distinct signals in response to joint movements. This suggests that the sensor can differentiate between various finger bending angles, thus making it applicable for recognizing sign language motions. The response speed of the Pt-b-A/W at 50 cpm is further evaluated by overlaying the voltage values at 30°, 60°, and 90° on the graph of bending angle (black line) in Figure 2g. Here, five cycles have been extracted from the same section for each bending angle. Notably, the voltage curves are seen to match the bending angle curve closely, thereby confirming the excellent responsiveness of the strain sensor to changes in angle. Moreover, although a response delay of about 0.1 s is observed for all three angle conditions, this will not lead to significant performance degradation in practical application because typical human movements occur at frequencies of 1 m/s [24]. Therefore, the sensor is able to measure joint motions in real time. The changes in output voltage of Pt-b-A/W during 1000 bending cycles to an angle of 90° at a fixed speed of 30 cpm are presented in Figure 2h. Here, the voltage exhibits a stable response without significant changes between the first and last five cycles, thereby demonstrating the excellent reproducibility and durability of the sensor.

Taken together, the above results indicate that the sensor with the plated structure provides excellent performance in terms of sensitivity, responsiveness, reliability, and reproducibility. This is

© 2025 by the author(s). Distributed under a Creative Commons CC BY license.

Preprints.org (www.preprints.org) | NOT PEER-REVIEWED | Posted: 16 June 2025 doi:10.20944/preprints202506.1182.v1

attributed to the effectiveness of the contact-separation mechanism when the conductive yarn is evenly distributed on the back side of the glove. Additionally, the absence of elastic yarn allows structural deformation to occur rapidly, thereby inducing numerous changes in contact points. Hence, the following section examines the practical application of a smart glove based on Pt-b-A/W for the recognition of KSL.

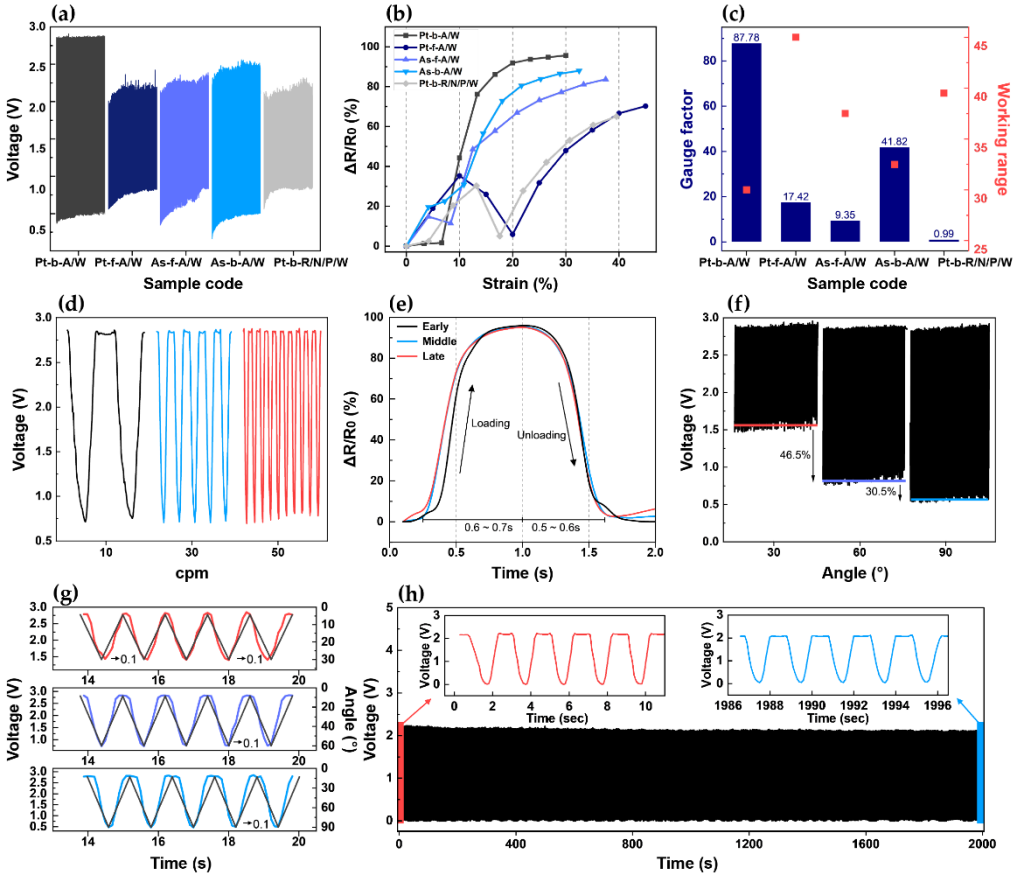

Figure 2. The dynamic bending test results for the five samples, along with an in-depth analysis of the results for Pt-b-A/W: (a) the voltage outputs of the five samples during 1000 bending cycles at 90°; (b) the relative resistance changes of the five samples at 90° and 30 cpm; (c) the corresponding GF values and working ranges; (d) the voltage fluctuations of the Pt-b-A/W according to bending speed at 90°; (e) the loading and unloading times at the beginning, middle, and end of 1000 cycles at 90° and 30 cpm; (f) the voltage outputs during 1000 cycles of bending to angles of 30°, 60°, and 90° at 50 cpm; (g) the voltage change at angles of 30°, 60°, and 90° at 50 rpm; and (h) the voltage changes during 1000 cycles at 90° and 30 cpm.

3.3. Development and Performance Evaluation of a KSL Smart Glove Translation System

3.3.1. Development

The design process and testing of the textile integration system for recognizing KSL gestures is shown in Figure 3. As shown in Figure 3a, the sensor was fabricated using a plain plated knit structure in which the conductive yarn is positioned on the back side of the fabric. The 3D structural representation on the right demonstrates how this configuration enables uniform loop deformation during stretching, thereby ensuring stable contact between conductive yarns.

Figure 3b depicts the wearable system, which integrates the sensor, signal wires, and snap connectors. With consideration for the finger area, sensors measuring 20 × 40 mm were placed at the center of the PIP joint. To detect independent movements of each finger, two signal lines were connected per finger, totaling 10 wires. These wires start from points 5 mm above and below the sensor and extend to the back of the hand. The circular snap buttons, each with a diameter of 5 mm, are attached at the ends of the wires and positioned at the center of the metacarpal bones to minimize discomfort during movement.

© 2025 by the author(s). Distributed under a Creative Commons CC BY license.

Preprints.org (www.preprints.org) | NOT PEER-REVIEWED | Posted: 16 June 2025 doi:10.20944/preprints202506.1182.v1

A photographic image of the as-fabricated KSL recognition smart glove is presented in Figure 3c. The glove integrates four components, namely: the knit sensor, interconnection lines, snap connectors, and MCU. The knit sensor is positioned on the inside surface of the glove to protect it from external contamination and physical damage. As the sensor is not externally exposed, the glove can be worn naturally during daily activities without compromising appearance or comfort. Additionally, the fabrication process is simple and fast, thus resulting in high production efficiency. The interconnection lines are fabricated with a zigzag stitch by using a sewing machine and is integrated with the glove, thus providing excellent wearing comfort without any sense of incongruity. The snap interconnector allows for easy attachment and detachment of the device to facilitate washing and maintenance of the gloves. The MCU is enclosed in a leather casing to protect it from external contaminants and scratches, while also enhancing the glove's aesthetic appeal and user-friendliness. Overall, the textile integration system was designed with key practical considerations in mind, including sensor protection, wearing comfort, ease of maintenance, and usability. Additionally, the straightforward fabrication process supports scalability and mass production. The process of recognizing KSL gestures using the developed smart glove is as follows: (1) the user wears the glove and performs sign language gestures by bending their fingers; (2) the degree of finger bending is detected by the integrated strain sensors; (3) the signals are processed by the MCU and interpreted as specific consonants or vowels; (4) the processed data are transmitted in real time to a smartphone via a BLE wireless communication module; and (5) the mobile application converts the received data into both voice and text to provide intuitive feedback to the user. The performance of this KSL smart glove motion recognition system is evaluated in the following section.

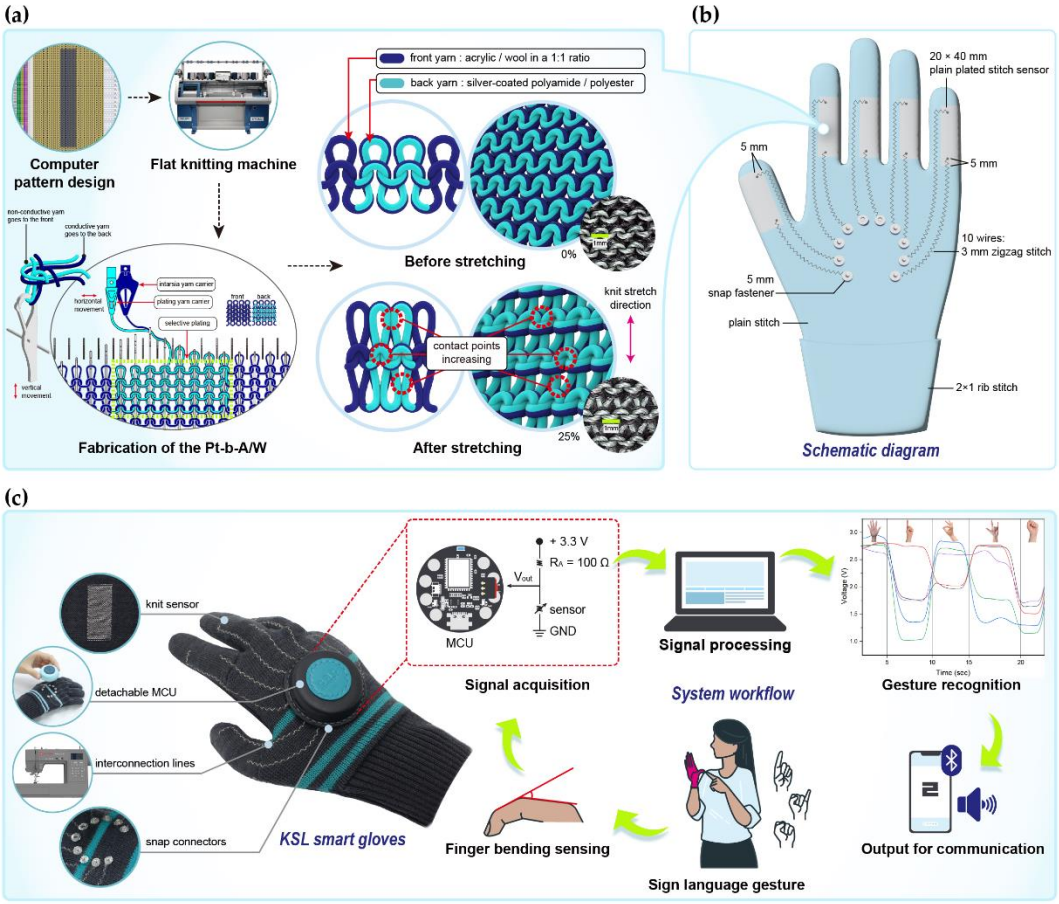

Figure 3. The fabrication, integration, and implementation of a smart glove for KSL gesture recognition: (a) fabrication of the plain plated stitch sensor and sensing mechanism; (b) a schematic diagram of the smart glove integrating the sensor, wires, and snap buttons; (c) A photographic image showing the process of recognizing KSL gestures using the as-developed smart glove.

© 2025 by the author(s). Distributed under a Creative Commons CC BY license.

Preprints.org (www.preprints.org) | NOT PEER-REVIEWED | Posted: 16 June 2025 doi:10.20944/preprints202506.1182.v1

3.3.2. Real-Time Performance Evaluation of the Smart Glove for KSL Fingerspelling

The voltage output signals obtained when performing fingerspelling motions while wearing the glove are shown in Figure 4, along with images displaying the corresponding real-time text and voice translations that are output through the mobile application. Before finger movement, the baseline output voltage ranges from 2.75 to 3.04 V (Figure 4a). When specific fingers are bent to represent Korean consonants and vowels, distinct voltage patterns are observed. For instance, during the 'ㄱ' motion involving the middle, ring, and little fingers, the voltage drops to 1.36, 1.37, and 1.58 V, respectively (Figure 4b). During the ‘ㄹ’ motion, which involves the thumb and little fingers, the voltage drops to 1.34 and 1.63 V, respectively (Figure 4c). For the ‘ㅁ’ motion, which involves all five fingers, the voltage drops to 0.94, 1.49, 1.43, 1.2 and 1.44 V, respectively (Figure 4d). During the ‘ㅂ’ motion, which involves only the thumb, the voltage drops to 1.24 V (Figure 4e). For the ‘ㅅ’ motion, which involves the thumb, ring finger, and little finger, the voltage drops to 1.04, 1.24 and 0.94 V, respectively (Figure 4f). The ‘ㅇ’ motion, which involves the thumb and index fingers, causes the voltage to drop to 1.8 and 1.63 V, respectively (Figure 4g). For the ‘ㅈ’ motion, which involves the ring and little fingers, the voltage drops to 1.62 and 1.23 V, respectively (Figure 4h). During the ‘ㅊ’ motion, which involves only the little finger, the voltage drops to 1.8 V (Figure 4i). For the ‘ㅋ’ motion, which involves the index, ring, and little fingers, the voltage drops to 1.95, 1.99, and 2.28 V, respectively (Figure 4j). The ‘ㅎ’ motion, which involves the index, middle, ring, and little fingers, causes the voltage to drop to 1.19, 1.61, 1.67, and 1.87 V, respectively (Figure 4k). When performing the ‘ㅏ’ motion, which involves the thumb, middle, ring, and little fingers, the voltage drops to 0.88, 1.51, 1.29, and 1 V, respectively (Figure 4l). Finally, the ‘ㅣ’ motion, which involves the thumb, index, middle and ring fingers, causes the voltage to drop to 0.96, 1.50, 1.47, and 1.71 V, respectively (Figure 4m). These consistent and simultaneous voltage responses confirm the sensor’s high reliability and rapid response during fingerspelling motions. In other words, these results demonstrate the structural excellence of the Pt-b-A/W sample and also confirm the practical feasibility of the textile integration system implemented using this fabric.

© 2025 by the author(s). Distributed under a Creative Commons CC BY license.

Preprints.org (www.preprints.org) | NOT PEER-REVIEWED | Posted: 16 June 2025 doi:10.20944/preprints202506.1182.v1

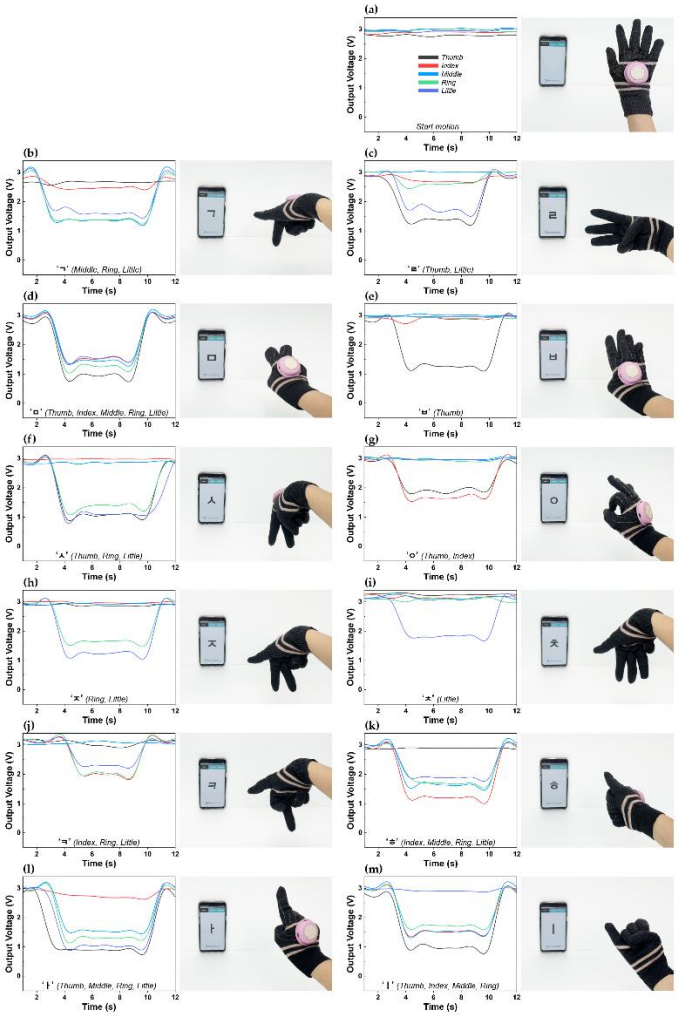

Figure 4. A demonstration of the knitted glove sensing system for the recognition of KSL hand motions using a wireless system: (a) start position; (b) motion 'ㄱ'; (c) motion 'ㄹ'; (d) motion 'ㅁ'; (e) motion 'ㅂ'; (f) motion 'ㅅ'; (g) motion 'ㅇ'; (h) motion 'ㅈ'; (i) motion 'ㅊ'; (j) motion 'ㅋ'; (k) motion 'ㅎ'; (l) motion 'ㅏ'; (m) motion 'ㅣ'.

4. Conclusions

This study investigated the relationship between the structural deformation mechanism and the electrical performance of knitted strain sensors, focusing on two key design variables: the placement of conductive yarn and the inclusion of elastic yarn. Among the five configurations evaluated, the plated structure with conductive yarn uniformly positioned on the back side and without elastic yarn (designated as Pt-b-A/W) demonstrated the most optimal performance for finger bending detection. This structure promoted uniform loop deformation and rapid structural responsiveness, resulting in superior sensor characteristics, including a gauge factor (GF) up to 89 times greater than those of other configurations. The sensor also maintained high performance across various bending angles and speeds.

Based on this optimized sensor, a smart glove system for Korean Sign Language (KSL) recognition was developed. The smart glove integrated the optimized knitted strain sensor with interconnection lines, snap connectors, and a microcontroller unit (MCU) to achieve excellent wearability, easy maintenance, and user convenience. The glove successfully recognized 12 KSL fingerspelling gestures in real time and translated them into both text and audio outputs via a smartphone application, thereby validating its practical feasibility.

Unlike previous studies, this work provides an in-depth analysis of how knitted structural design directly influences sensor performance and extends these findings into a fully integrated wearable system. The as-developed high-performance sensor can be applied to various parts of the body, thus making it promising for a wide range of applications such as healthcare, rehabilitation,

© 2025 by the author(s). Distributed under a Creative Commons CC BY license.

Preprints.org (www.preprints.org) | NOT PEER-REVIEWED | Posted: 16 June 2025 doi:10.20944/preprints202506.1182.v1

and human–computer interaction. Moreover, the modular design of the textile-integrated system offers scalability and supports mass production, suggesting a viable commercialization path for next-generation wearable technologies.

References

1. Cipolla, R., & Pentland, A. (1998). *Computer vision for human-machine interaction*. Cambridge University Press.
2. Hill, J. C., Lillo-Martin, D. C., & Wood, S. K. (2019). *Sign languages: Structures and contexts* (1st ed., Chap. 1). Routledge.
3. Lane, H. (1992). Mask of benevolence: Disabling the Deaf community. Knopf.
4. Roh, J. S. (2016). Wearable textile strain sensors. *Fashion & Textile Research Journal*, 18(6), 734–736. https://doi.org/10.5805/sfti.2016.18.6.733
5. Ryu, H., Park, S., Park, J.-J., & Bae, J. (2018). A knitted glove sensing system with compression strain for finger movements. *Smart Materials and Structures*, 27(5), 055016. https://doi.org/10.1088/1361-665X/aab7cc
6. Heo, J. S., Shishavan, H. H., Soleymanpour, R., Kim, J., & Kim, I. (2020). Textile-based stretchable and flexible glove sensor for monitoring upper extremity prosthesis functions. *IEEE Sensors Journal*, 20(4), 1754–1760. https://doi.org/10.1109/JSEN.2019.2949177
7. Lee, S., Choi, Y., Sung, M., Bae, J., & Choi, Y. (2021). A knitted sensing glove for human hand postures pattern recognition. *Sensors*, 21(4), 1364. https://doi.org/10.3390/s21041364
8. Han, X., Miao, X., Liu, Q., Li, Y., & Wan, A. (2022). A fabric-based integrated sensor glove system recognizing hand gesture. *Autex Research Journal*, 22(4), 458–465. https://doi.org/10.2478/aut-2021-0016
9. Qin, Y., Wang, T., Li, X., Wang, H., & Guo, X. (2025). The woven fabric sensor and the intelligent glove based on eco-flex/carbon composite ink. *FlexTech*, 1(1), 53–62. https://doi.org/10.1002/fle2.12010
10. Cheng, X., Shen, D., Zheng, K., Wu, Z., Shi, L., & Hu, X. (2025). A wearable strain sensor for medical rehabilitation based on piezoresistive knitting textile. *Sensors and Actuators A: Physical*, 387, 116379. https://doi.org/10.1016/j.sna.2025.116379
11. Park, S. Y. (2022). *Development of finger motion recognition gloves using knit-type strain sensors* (Master's thesis, Kookmin University, Seoul, Republic of Korea).
12. Oh, Y.-K., & Kim, Y.-H. (2024). Evaluation of electrical characteristics of weft-knitted strain sensors for joint motion monitoring: Focus on plating stitch structure. *Sensors*, 24(23), 7581. https://doi.org/10.3390/s24237581
13. Kim, J. S. (2014). Pattern design by knitting structure and properties. *Korea Society of Design Trend*, 45, 480–481. https://doi.org/10.21326/ksdt.2014..45.042
14. Hong, M. H., & Choi, K. M. (2009). *Knit design guidebook*. Kcpub.
15. Tohidi, S. D., Zille, A., Catarino, A. P., & Rocha, A. M. (2018). Effects of base fabric parameters on the electro-mechanical behavior of piezoresistive knitted sensors. *IEEE Sensors Journal*, 18(11), 4529–4535. https://doi.org/10.1109/JSEN.2018.2826056
16. Atalay, O., Kennon, W. R., & Husain, M. D. (2013). Textile-based weft knitted strain sensors: Effect of fabric parameters on sensor properties. *Sensors*, 13(8), 11114–11127. https://doi.org/10.3390/s130811114
17. Stoll GmbH & Co. KG. (2013). *Stoll training manual: Flat knitting machine* (Ident-No. 223 788_01). Stoll GmbH & Co. KG.
18. Jo, D. B. (2021). Development of wearable smart gloves and sign language translation system using conductive polymer composite strain sensor (Master's thesis, Hanyang University, Seoul, Republic of Korea).
19. Kim, J., & Kang, E. (2022). Korean finger spelling recognition using hand landmarks. *The Journal of Korean Institute of Next Generation Computing*, 18(1), 81–91.
20. Lee, J. W., & Nam, K. H. (2014). *Korean sign language linguistics*. Nanam.
21. Rumon, M. A. A., Cay, G., Ravichandran, V., Altekreeti, A., Gitelson-Kahn, A., Constant, N., Solanki, D., & Mankodiya, K. (2023). Textile knitted stretch sensors for wearable health monitoring: Design and performance evaluation. *Biosensors*, 13(1), 34. https://doi.org/10.3390/bios13010034

© 2025 by the author(s). Distributed under a Creative Commons CC BY license.

Preprints.org (www.preprints.org) | NOT PEER-REVIEWED | Posted: 16 June 2025 doi:10.20944/preprints202506.1182.v1

22. Jang, J. H., Kim, S. J., Lee, K. M., Park, S. J., Park, G. Y., Kim, B. J., Oh, J. H., & Lee, M. J. (2021). Knitted strain sensor with carbon fiber and aluminum-coated yarn for wearable electronics. *Journal of Materials Chemistry C*, 9, 16440–16449. https://doi.org/10.1039/D1TC01899J
23. Cieślik, K., & Łopatka, M. J. (2022). Research on speed and acceleration of hand movements as command signals for anthropomorphic manipulators as a master-slave system. *Applied Sciences*, 12(8), 3863. https://doi.org/10.3390/app12083863

Disclaimer/Publisher's Note: The statements, opinions and data contained in all publications are solely those of the individual author(s) and contributor(s) and not of MDPI and/or the editor(s). MDPI and/or the editor(s) disclaim responsibility for any injury to people or property resulting from any ideas, methods, instructions or products referred to in the content.

© 2025 by the author(s). Distributed under a Creative Commons CC BY license.